Self-Ordered Aluminum Anodizing in Phosphonoacetic Acid and Its Structural Coloration

Akimasa Takenaga, Tatsuya Kikuchi,[z] Shungo Natsui, and Ryosuke O. Suzuki

Faculty of Engineering, Hokkaido University, Sapporo, Hokkaido, 060-8628, Japan

Ordered anodic porous alumina with large-scale periodicity was fabricated via phosphonoacetic acid anodizing. Aluminum specimens were anodized in a 0.1–0.9 M phosphonoacetic acid solution under various electrochemical operating conditions, and optimum anodizing at 205–225 V exhibited self-ordering growth of the porous alumina. These self-ordering voltages during phosphonoacetic acid anodizing filled an undiscovered vacant region in the linear relationship between the self-ordering voltage and the cell diameter. The nanostructured aluminum surface formed via self-ordering phosphonoacetic acid anodizing produced a bright structural coloration with a visible light wavelength of 500–700 nm, which is useful for optical nanoapplications.
 [DOI: 10.1149/2.0021508ssl]

Manuscript submitted May 8, 2015; revised manuscript received May 26, 2015. Published June 4, 2015.

Self-ordered anodic porous alumina possesses a well-defined periodic porous structure with numerous nanopores that have high aspect ratios.[1–3] This characteristic nanoporous material is widely used for various novel nanoapplications, including electronic, optical, and sensing devices.[4–12] Ordered porous alumina can be fabricated by electrochemical anodizing in several acidic electrolyte solutions under appropriate experimental conditions such as concentration and applied voltage. The periodical size of the obtained ordered porous alumina, defined as the "cell size" or "interpore distance", is typically determined by the electrolyte species used.[2,3,13] In self-ordered anodizing, the regularity of the pore arrangement in the porous structure can be accurately determined by a quantitative analysis based on Fourier transformation.[14–19] Sulfuric, oxalic, and phosphoric acids were found early and have been commonly used as the standard self-ordering electrolytes to date.[13,20,21] However, the cell size of these ordered porous alumina is limited to the following narrow nanometer-scale regions: 50–60 nm in sulfuric acid, 100 nm in oxalic acid, and 405–500 nm in phosphoric acid.[13] Therefore, the identification of novel electrolytes for self-ordered porous alumina with different cell sizes has been a recent challenge to extensively expand the nano-periodicity. Additional dicarboxylic acids with a large molecular structure, malonic and tartaric acids, for the fabrication of anodic porous alumina were reported by Ono et al., and self-ordering was achieved by anodizing with these acids for 300 and 500 nm intervals, respectively.[22]

Recently, we reported several novel electrolytes for the formation of anodic porous alumina: selenic,[23,24] acetylenedicarboxylic,[25] squaric,[26] croconic,[27] rhodizonic,[27] ketoglutaric,[28] acetonedicarboxylic,[28] and etidronic acids.[29,30] Particularly, etidronic acid anodizing exhibited large-scale self-ordering behavior measuring 530–670 nm in cell diameter. Etidronic acid is one of the most popular phosphonates for medicines, washing agents, and inhibitors, and many other phosphonate molecules are also commercially available for industrial and medical applications. Therefore, it is expected that anodizing in these phosphonate electrolytes may also exhibit different self-ordering behaviors of porous alumina.

Herein, we reported the fabrication of self-ordered porous alumina via anodizing in a new electrolyte, phosphonoacetic acid ($C_2H_5O_5P$, $(HO)_2P(O)CH_2COOH$). Ordered porous alumina measuring 500–550 nm in cell diameter was successfully fabricated via phosphonoacetic acid anodizing, and the nanostructured aluminum surface produced a bright structural coloration.

Experimental

High-purity aluminum plates (99.999 wt%, GoodFellow, UK) were ultrasonically degreased in ethanol for 10 min and then were electropolished in a 13.6 M CH_3COOH/2.56 M $HClO_4$ (78 vol% CH_3COOH/22 vol% 70% $HClO_4$) mixture at 28 V for 1 min. The electropolished aluminum specimens were immersed in a 0.1–0.9 M phosphonoacetic acid solution (Wako Pure Chemical Industries, Japan, T = 273–323 K) and were anodized at a constant cell voltage of U = 205–245 V for 180 min. During anodizing, the voltage increased linearly for first 2.5 min and then was held constant using a direct current power supply (PWR-400H, Kikusui, Japan). A high-purity platinum plate was used as the counter electrode, and the solution was vigorously stirred with a magnetic stirrer during anodizing to avoid the oxide burning phenomena as much as possible. After anodizing, the oxide film was selectively dissolved from the aluminum substrate in a 0.2 M CrO_3/0.51 M H_3PO_4 solution (T = 353 K). Therefore, the nanostructured aluminum, corresponding to the interface between the anodic oxide and the aluminum substrate, was exposed to the surface of the specimen.

The anodized specimens were examined by field emission scanning electron microscopy (FE-SEM, JSM-6500F and JIB-4600F/HKD, JEOL, Japan). Optical reflectance measurement of the nanostructured aluminum surface was also performed using a multi-channel spectrometer and a white light source (USB2000+ and HL-2000, Ocean Optics, USA) through an optical fiber.

Results and Discussion

Figures 1a–1c show the changes in the current density, j, with anodizing time, t, at various constant voltages in a 0.1–0.9 M phosphonoacetic acid solution at 283 K. In 0.3 M phosphonoacetic acid (Fig. 1a), the following typical current-time transients were measured during anodizing at applied voltages of 210–225 V: i) rapid increase and subsequent decrease after the voltage was applied within 2.5 min due to the barrier oxide formation on the aluminum substrate, ii) rapid increase again after approximately 40 min due to the initiation of nanopores formation in the anodic oxide, and iii) gradual decrease and steady current density due to the steady-state growth of the porous alumina. In contrast, the current density at the high voltage of 230 V rapidly increased to above 100 Am^{-2} after 40 min of anodizing because the oxide burned due to high current density in localized regions, which was caused by the high applied electric field. Non-uniform anodic oxide with dark brown color was formed by anodizing over the limit of applied voltage.[31,32] The peak current density without oxide burning increased with applied voltage, and the most rapid oxide growth was expected by anodizing at the highest voltage of 225 V. An SEM image of the fracture cross-section of the specimen anodized at 225 V is shown in Figure 1d. Many nanopores several tens of nanometers in diameter were formed on the surface, and an anodic porous alumina with 100-nm-scale pores grew vertically from

[z]E-mail: kiku@eng.hokudai.ac.jp

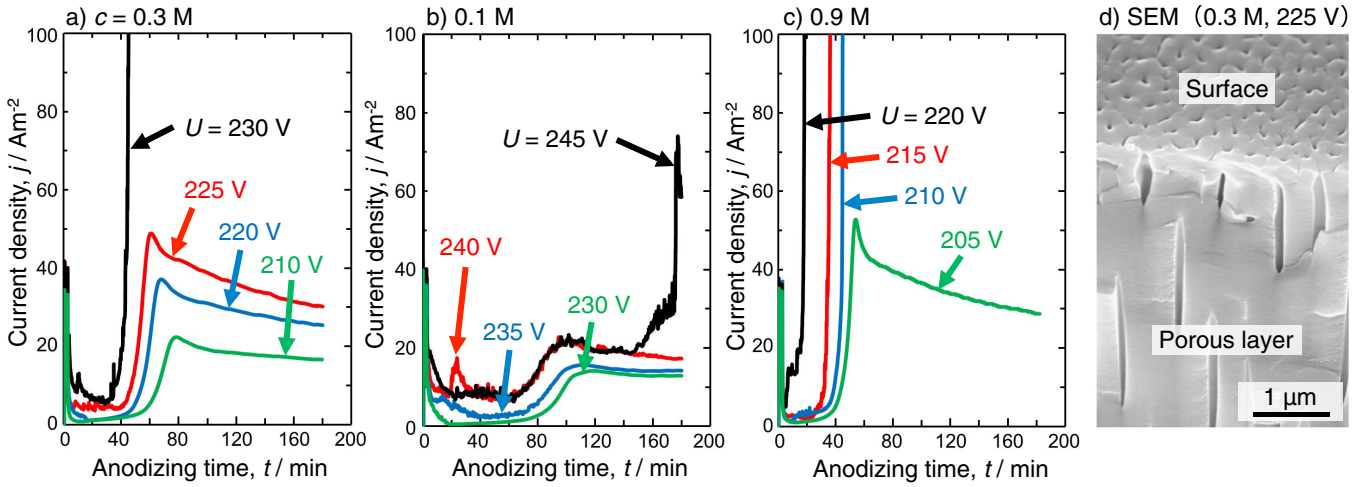

Figure 1. The change in the current density, j, with time, t, during anodizing in a) 0.3 M, b) 0.1 M, and c) 0.9 M phosphonoacetic acid solutions at different applied voltages of $U = 205$–245 V. d) SEM image of the fracture cross-section of the specimen anodized at 225 V for 180 min.

the surface of the specimen. It was clear from these investigations that phosphonoacetic acid anodizing created an anodic porous alumina, and thus revealed that phosphonoacetic acid has the potential to be a new electrolyte for the fabrication of anodic porous alumina.

As the concentration decreased to 0.1 M (Fig. 1b), the maximum applied voltage without oxide burning increased to 240 V from 225 V. However, the current density was much lower than that obtained in 0.3 M phosphonoacetic acid, and thus it was expected that the growth rate of the porous alumina was much slower than that of 0.3 M phosphonoacetic acid. When the concentration increased to 0.9 M (Fig. 1c), on the other hand, the peak current density without oxide burning exhibited a relatively high value, although the maximum voltage without oxide burning decreased to 205 V in 0.9 M phosphonoacetic acid (Fig. 1c). From these electrochemical measurements, the following important behaviors could be summarized: a) the highest anodizing voltage without oxide burning decreased with increasing the phosphonoacetic acid concentration and b) the current density at the highest voltage increased with increasing the concentration. Therefore, the growth rate of the anodic oxide increased with the concentration.

The porous alumina anodized in the different conditions mentioned above was selectively dissolved in a CrO_3/H_3PO_4 solution for regularity analysis. Figures 2a–2c show the SEM images of the nanostructured aluminum surface anodized in a 0.3 M phosphonoacetic acid solution at 283 K and 210–225 V for 180 min. At 210 V, a disordered aluminum dimple array measuring approximately 530 nm in diameter was distributed on the aluminum surface. The regularity of the dimple array slightly improved with applied voltage, and a relatively well-ordered dimple array with a diameter of approximately 550 nm was observed on the aluminum anodized at the maximum voltage of 225 V (Fig. 2c). This improved behavior via maximum high-voltage anodizing without oxide burning can typically be observed during the self-ordering of porous alumina.[29] Such self-ordering behavior is achieved by the highly viscous flow of the anodic oxide under high current density/growth rate conditions.[22,33,34]

In a 0.1 M phosphonoacetic acid solution at 240 V (Fig. 2d), the size of the dimples slightly increased due to the high applied voltage; however, a disordered dimple array was observed on the aluminum surface. It was difficult to obtain ordered porous alumina via phosphonoacetic acid anodizing in such low concentration under whole anodizing conditions because of the low current density during anodizing. Conversely, the regularity of the dimple array improved as the concentration increased. An ordered aluminum dimple array of 500 nm in dimple diameter was obtained on the aluminum surface anodized in a 0.9 M phosphonoacetic acid solution at 205 V (Fig. 2e), although several defects and non-hexagonal dimples still remained in the arrangement. Through phosphonoacetic acid anodizing, a high solution concentration easily caused the formation of an ordered dimple array due to the high current density and highly viscous flow. Various constant voltage anodizing processes were explored at different solution temperatures from 273–323 K. As a result, it was found that the temperatures from 283–288 K were the most suitable conditions for ordered porous alumina fabrication during phosphonoacetic acid anodizing (Fig. 2f, cell diameter: 515 nm).

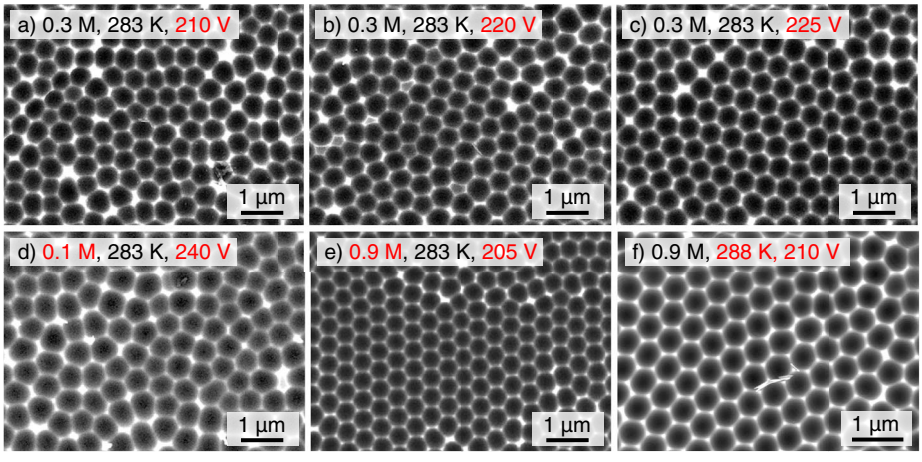

Figure 2. SEM images of the nanostructured aluminum surface fabricated via phosphonoacetic acid anodizing under various operating conditions and subsequent selective oxide dissolution.

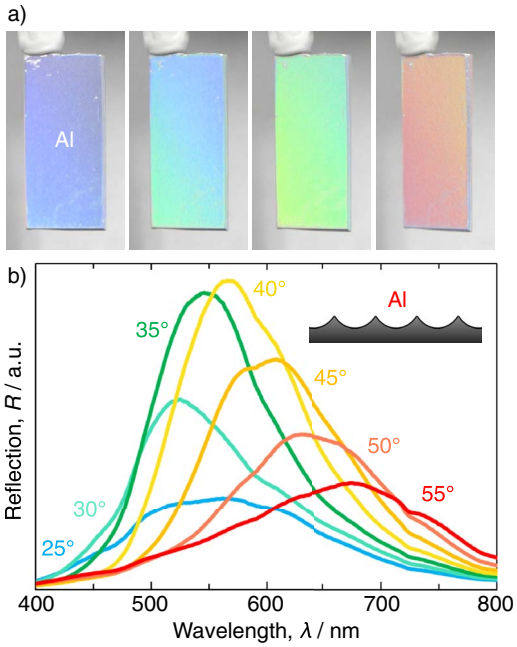

Figure 3. a) Surface appearances of the nanostructured aluminum specimen anodized in phosphonoacetic acid solution at 205 V for 180 min at different viewing angles. b) Reflection spectrum from the nanostructured aluminum surface with viewing angles of 25–55° under white light irradiation.

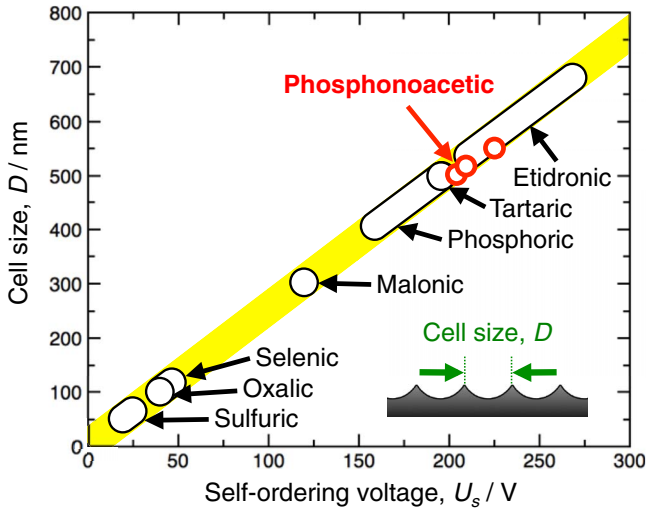

Figure 4. The linear relationship of the cell diameter, D, with the self-ordering voltage, U_s, for the fabrication of highly ordered anodic porous alumina in various aqueous electrolyte solutions.

The nanostructured aluminum surface with honeycomb distribution obtained by phosphonoacetic acid anodizing exhibited the characteristic bright rainbow distribution under white light irradiation. Figure 3a shows the surface appearances of the nanostructured aluminum specimen via phosphonoacetic acid anodizing at 205 V and different viewing angles. The aluminum surface clearly exhibited bright structural colors including violet, aqua blue, light green, and red hues. Such structural coloration was generated by the interference from the periodically ordered aluminum dimple array with large-scale cell diameters.[29,30] Therefore, it could be determined that the dimple array formed via phosphonoacetic acid anodizing has good regularity on the entire surface of the specimen. Figure 3b shows the changes in the reflection spectrum, *R*, from the nanostructured aluminum surface at different angles under white light irradiation. The selective color reflections were measured at approximately 500–700 nm. In particular, the lights were strongly reflected in the green and yellow wavelengths, which their wavelengths were similar to the intervals (i.e., cell diameter) of the ordered dimple arrays. The structural coloration based on the ordered dimple array could be employed in various optical applications and as the templates for optical devices.

The self-ordering voltage of the porous alumina, U_s, and the corresponding cell diameter, *D*, obtained via anodizing in phosphonoacetic acid, as well as previously reported various electrolytes, are summarized in Figure 4. The linear relationship between the voltage and cell diameter during self-ordering anodizing in aqueous solutions is described, and phosphonoacetic acid anodizing provided the self-ordering region of approximately 500–550 nm at 205–225 V. Although the window of this self-ordering behavior is slightly narrow, the vacancy gap between phosphoric acid and etidronic acid is filled by phosphonoacetic acid anodizing. Moreover, it was found that the nanostructured aluminum surface with this cell diameter exhibited the characteristic structural coloration based on the interference from the ordered nanostructure. On the other hand, the self-ordering region by anodizing in etidronic acid was wider than that obtained in phosphonoacetic acid, which is a relatively high-cost electrolyte in commercial terms.

In summary, we have demonstrated that phosphonate electrolytes have the potential to behave as suitable electrolytes for the fabrication of porous alumina, similar to carboxylic and oxocarbon acid groups. Through further investigations, additional phosphonate electrolytes will be found for porous alumina with different and characteristic nanomorphologies.

Conclusions

Aluminum anodizing in phosphonoacetic acid solutions under various electrochemical operating conditions was described in the present study. Ordered porous alumina measuring approximately 500–550 nm in cell diameter could be successfully fabricated via phosphonoacetic acid anodizing at 205–225 V. The nanostructured aluminum surface formed via self-ordered phosphonoacetic acid anodizing and subsequent selective oxide dissolution exhibited bright structural coloration measuring 500–700 nm in the visible light wavelength.

Acknowledgments

This study was conducted at Hokkaido University and was supported by the "Nanotechnology Platform" Program of the Ministry of Education, Culture, Sports, Science, and Technology (MEXT), Japan. The work was financially supported by the Light Metal Educational Foundation and the Japan Society for the Promotion of Science (JSPS) "KAKENHI".

References

1. F. Keller, M. S. Hunter, and D. L. Robinson, *J. Electrochem. Soc.*, **100**, 411 (1953).
2. W. Lee and S. J. Park, *Chem. Rev.*, **114**, 7487 (2014).
3. G. D. Sulka, in *Nanostructured Materials in Electrochemistry*, A. Eftekhari, Editor, P. 1, Wiley-VCH, Weinheim (2008)
4. D. N. Kelly, R. H. Wakabayashi, and A. M. Stacy, *ACS Appl. Mater. Interfaces*, **6**, 20122 (2014).
5. T. Ozel, G. R. Bourret, and C. A. Mirkin, *Nat. Nanotechnol.*, **10**, 319 (2015).
6. J. Martín, M. Martín-González, J. F. Fernández, and O. Caballero-Calero, *Nat. Commun.*, **5**, 5130 (2014).
7. S. Z. Kure-Chu, K. Osaka, H. Yashiro, H. Segawa, K. Wada, and S. Inoue, *J. Electrochem. Soc.*, **162**, C24 (2015).
8. C. Yang, Y. Qin, X. Zhu, M. Yin, D. Lin, X. Chen, and Y. Song, *J. Alloys Compd.*, **632**, 634 (2015).
9. T. Yanagishita, M. Masui, N. Ikegawa, and H. Masuda, *J. Vac. Sci. Technol. B*, **32**, 021809 (2014).
10. Q. Lin, B. Hua, S. Leung, X. Duan, and Z. Fan, *ACS Nano*, **7**, 2725 (2013).
11. T. Kawasaki, *J. Electrostat.*, **66**, 295 (2008).
12. K. H. Lee, Y. P. Huang, and C. C. Wong, *Electrochim. Acta*, **56**, 2394 (2011).
13. W. Lee, R. Ji, U. Gösele, and K. Nielsch, *Nat. Mater.*, **5**, 741 (2006).
14. W. J. Stępniowski, D. Forbot, M. Norek, M. Michalska-Domańska, and A. Król, *Electrochim. Acta*, **133**, 57 (2014).

15. W. J. Stępniowski, A. Nowak-Stępniowska, and Z. Bojar, *Mater. Charact.*, **78**, 79 (2013).
16. L. Zaraska, W. J. Stępniowski, E. Ciepiela, and G. D. Sulka, *Thin Solid Films*, **534**, 155 (2013).
17. W. J. Stępniowski and Z. Bojar, *Surf. Coat. Technol.*, **206**, 265 (2011).
18. I. Turkevych, V. Ryukhtin, V. Garamus, S. Kato, T. Takamasu, G. Kido, and M. Kondo, *Nanotechnology*, **23**, 325606 (2012).
19. L. Zaraska, G. D. Sulka, J. Szeremeta, and M. Jaskuła, *Electrochim. Acta*, **55**, 4377 (2010).
20. A. P. Li, F. Müller, A. Birner, K. Nielsch, and U. Gösele, *J. Appl. Phys.*, **84**, 6023 (1998).
21. K. H. Lee and C. C. Wong, *J. Appl. Phys.*, **106**, 104305 (2009).
22. S. Ono, M. Saito, and H. Asoh, *Electrochim. Acta*, **51**, 827 (2005).
23. O. Nishinaga, T. Kikuchi, S. Natsui, and R. O. Suzuki, *Sci. Rep.*, **3**, 2748 (2013).
24. T. Kikuchi, O. Nishinaga, S. Natsui, and R. O. Suzuki, *Electrochim. Acta*, **137**, 728 (2014).
25. T. Kikuchi, O. Nishinaga, S. Natsui, and R. O. Suzuki, *ECS Electrochem. Lett*, **3**, C25 (2014).
26. T. Kikuchi, T. Yamamoto, S. Natsui, and R. O. Suzuki, *Electrochim. Acta*, **123**, 14 (2014).
27. T. Kikuchi, D. Nakajima, J. Kawashima, S. Natsui, and R. O. Suzuki, *Appl. Surf. Sci.*, **313**, 276 (2014).
28. D. Nakajima, T. Kikuchi, J. Kawashima, S. Natsui, and R. O. Suzuki, *Appl. Surf. Sci.*, **321**, 364 (2014).
29. T. Kikuchi, O. Nishinaga, S. Natsui, and R. O. Suzuki, *Electrochim. Acta*, **156**, 235 (2015).
30. T. Kikuchi, O. Nishinaga, S. Natsui, and R. O. Suzuki, *Appl. Surf. Sci.*, **341**, 19 (2015).
31. T. Aerts, I. D. Graeve, and H. Terryn, *Electrochim. Acta*, **54**, 270 (2008).
32. S. Ono, M. Saito, M. Ishiguro, and H. Asoh, *J. Electrochem. Soc.*, **151**, B473 (2004).
33. J. E. Houser and K. R. Hebert, *Nat. Mater.*, **8**, 415 (2009).
34. Ö. Ö. Çapraz, P. Shrotriya, P. Skeldon, G. E. Thompson, and K. R. Hebert, *Electrochim. Acta*, **167**, 404 (2015).